

Thermal nuclear pairing within the self-consistent quasiparticle RPA

N. Dinh Dang^{1,2} and N. Quang Hung^{1,3}

¹ Theoretical Nuclear Physics Laboratory, RIKEN Nishina Center for Accelerator-Based Science, 2-1 Hirosawa, Wako City, 351-0198 Saitama, Japan

² Institute for Nuclear Science and Technique, Hanoi, Vietnam

³ Institute of Physics, Hanoi, Vietnam

E-mail: dang@riken.jp (N.D.D.), nqhung@riken.jp (N.Q.H.)

Abstract. The self-consistent quasiparticle RPA (SCQRPA) is constructed to study the effects of fluctuations on pairing properties in nuclei at finite temperature and z -projection M of angular momentum. Particle-number projection (PNP) is taken into account within the Lipkin-Nogami method. Several issues such as the smoothing of superfluid-normal phase transition, thermally assisted pairing in hot rotating nuclei, extraction of the nuclear pairing gap using an improved odd-even mass difference are discussed. A novel approach of embedding the PNP SCQRPA eigenvalues in the canonical and microcanonical ensembles is proposed and applied to describe the recent empirical thermodynamic quantities for iron, molybdenum, dysprosium, and ytterbium isotopes.

1. Introduction

Sharp phase transitions such as the superfluid-normal (SN) or shape ones are prominent features of infinite systems such as metal superconductors, ultra-cold gases, liquid helium, etc. They are well described by many-body theories such as the BCS, RPA or quasiparticle RPA (QRPA). The situation changes in finite small systems such as atomic nuclei, where strong quantal and thermal fluctuations strongly or completely smooth out these sharp phase transitions. It is well known that the conventional BCS, RPA or QRPA theories fail in a number of cases in the description of the ground states as well as excited states of these systems. The reason is that strong fluctuations invalidate the assumptions, based on which the main equations of these theories have been derived. Amongst these assumptions are the Cooper pairs, which violate the particle-number conservation, and the closely related quasiboson-approximation (QBA) used in the (Q)RPA, which violates the Pauli principle between the fermion pairs. These assumptions cause the BCS and QRPA to break down at a certain critical value G_c of the pairing interaction parameter G , below which the BCS theory only has a trivial solution with zero pairing gap $\Delta = 0$. The same is true in the weak coupling region, where the particle-particle RPA is valid but its solution also breaks down at $G \geq G_c$. Meanwhile, the exact solution of the pairing problem exposes no singularity at any G [1]. Similarly, at finite temperature $T \neq 0$, the omission of quasiparticle-number fluctuations (QNF) within the BCS theory leads to the collapse of the pairing gap at the critical temperature T_c , corresponding to the temperature of the SN phase transition in infinite systems. Meanwhile, the exact eigenvalues of the pairing problem embedded in the canonical ensemble (CE) shows a smooth decreasing pairing energy with increasing T due

to thermal fluctuations incorporated in the CE [2]. In rotating nuclei, strong fluctuations also smear out the Mottelson-Valatin effect, according to which the pairing gap, existing at zero angular momentum $M = 0$, would collapse at a certain critical angular momentum M_c . This situation means that, in order to be reliable, the BCS, RPA, and/or QRPA theories need to be corrected to include these effects of fluctuations when applied to nuclei, in particular, the light ones. This is done within the framework of the self-consistent QRPA (SCQRPA) presented in this work.

2. Formalism

We consider the pairing Hamiltonian $H = \sum_{k>0} \epsilon_k \hat{N}_{\pm k} - G \sum_{kk'} \hat{P}_k^\dagger \hat{P}_{k'}$, where $\hat{N}_{\pm k} = a_{\pm k}^\dagger a_{\pm k}$ is the particle-number operator, and $\hat{P}_k = a_k^\dagger a_{-k}^\dagger$, $\hat{P}_j = (\hat{P}_j^\dagger)^\dagger$ are the pairing operators. The operators a_k^\dagger and a_k are respectively the single-particle creation and destruction operators. This Hamiltonian has been diagonalized exactly in [1]. The exact partition function is constructed by embedding the exact eigenvalues into the CE as $Z_{\text{Exact}}(\beta) = \sum_S d_S \exp(-\beta \varepsilon_S^{\text{Exact}})$, with the degeneracy $d_S = 2^S$, inverse temperature $\beta = 1/T$, and $S = 0, 2, \dots, N$ being the total seniority of the system. Knowing the partition function Z , one calculates the free energy F , entropy S , total energy \mathcal{E} , heat capacity C , and pairing gap Δ as $F = -T \ln Z(T)$, $S = -\partial F / \partial T$, $\mathcal{E} = F + TS$, $C = \partial \mathcal{E} / \partial T$, and $\Delta = [-G(\mathcal{E} - 2 \sum_k \epsilon_k f_k + G \sum_k f_k^2)]^{1/2}$, where f_k is the single-particle occupation number on the k th level obtained by averaging the state-dependent occupation numbers $f_k^{(S)}$ within the CE [2].

The SCQRPA theory [3, 4] includes a set of BCS-based equations, corrected by the effects of QNF, namely

$$\Delta_k = \Delta + \delta\Delta_k, \quad \Delta = G \sum_{k'} \langle \mathcal{D}_{k'} \rangle u_{k'} v_{k'}, \quad \delta\Delta_k = 2G \frac{\delta \mathcal{N}_k^2}{\langle \mathcal{D}_k \rangle} u_k v_k. \quad (1)$$

$$N = 2 \sum_k \left[v_k^2 \langle \mathcal{D}_k \rangle + \frac{1}{2} (1 - \langle \mathcal{D}_k \rangle) \right]. \quad (2)$$

where u_k and v_k are the Bogoliubov's coefficients,

$$u_k^2 = \frac{1}{2} \left(1 + \frac{\epsilon'_k - G v_k^2 - \lambda}{E_k} \right), \quad v_k^2 = \frac{1}{2} \left(1 - \frac{\epsilon'_k - G v_k^2 - \lambda}{E_k} \right), \quad E_k = \sqrt{(\epsilon'_k - G v_k^2 - \lambda)^2 + \Delta_k^2}, \quad (3)$$

with the renormalized single-particle energies ϵ'_k

$$\epsilon'_k = \epsilon_k + \frac{G}{\langle \mathcal{D}_k \rangle} \sum_{k'} (u_{k'}^2 - v_{k'}^2) \left(\langle \mathcal{A}_k^\dagger \mathcal{A}_{k' \neq k}^\dagger \rangle + \langle \mathcal{A}_k^\dagger \mathcal{A}_{k'} \rangle \right), \quad (4)$$

$\langle \mathcal{D}_k \rangle = 1 - 2n_k$, the quasiparticle-pair operators $\mathcal{A}_k^\dagger = \alpha_k^\dagger \alpha_{-k}^\dagger$, $\mathcal{A}_k = (\mathcal{A}_k^\dagger)^\dagger$, and $\delta \mathcal{N}_k^2 \equiv n_k(1 - n_k)$ is the QNF on k th level. To avoid level-dependent gaps Δ_k , the level-weighted gap $\bar{\Delta}_k = \sum_k \Delta_k / \Omega$ (Ω is the number of levels) is considered in the numerical results. Because of coupling to collective vibrations beyond the quasiparticle mean field, the quasiparticle occupation number n_k is not given by a Fermi-Dirac distribution of free fermions, but is found from the integral equation [4]

$$n_k = \frac{1}{\pi} \int_{-\infty}^{\infty} \frac{\gamma_k(\omega) (e^{\beta\omega} + 1)^{-1}}{[\omega - E_k - M_k(\omega)]^2 + \gamma_k^2(\omega)} d\omega, \quad (5)$$

where the mass operator $M_k(\omega)$ and the quasiparticle damping $\gamma_k(\omega)$ are functions of n_k , SCQRPA eigenvalues ω_μ , SCQRPA \mathcal{X}_k^μ and \mathcal{Y}_k^μ amplitudes, SCQRPA phonon occupations

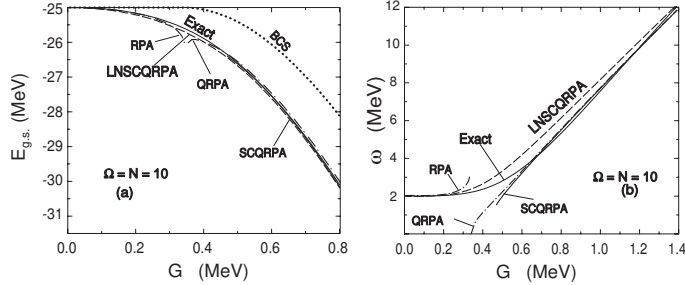


Figure 1. Energies of the ground state (a) and first excited states for the $N = \Omega = 10$ as functions of G at $T = M = 0$. $\omega_{ppRPA} = \mathcal{E}_1(N+2) - \mathcal{E}_0(N+2)$ with the ppRPA eigenvalues \mathcal{E}_i .

numbers ν_μ , as well as u_k and v_k . The SCQRPA submatrices A and B contain the screening factors $\langle \mathcal{A}_k^\dagger \mathcal{A}_{k'}^\dagger \rangle$ and $\langle \mathcal{A}_k^\dagger \mathcal{A}_{k'} \rangle$ so that the set of SCQRPA equations should be solved self-consistently with Eqs. (1), (2) and (5) to simultaneously determine $\bar{\Delta}$, chemical potential λ , n_k , ω_μ , \mathcal{X}_k^μ and \mathcal{Y}_k^μ . To eliminate particle-number fluctuations inherent in the BCS theory, the Lipkin-Nogami (LN) particle-number projection (PNP) [5] is applied on top of Eqs. (1) and (2). The ensuing theory, called the LNSQRPA theory, has also been extended to include the finite z -projection M of angular momentum (noncollective rotation) [6]. The set of obtained equations is formally the same except that now, depending on the single-particle spin projections $\mp \gamma m_k$ with γ being the angular velocity, one has two types of quasiparticle occupation number, n_k^\pm , so that $\langle \mathcal{D}_k \rangle = 1 - n_k - n_{-k}$. At $T = 0$ and $M = 0$ the SCQRPA theory reduces to its zero temperature and non-rotating limit, where $\langle \mathcal{D}_k \rangle = 1/[1 + 2 \sum_\mu (\mathcal{Y}_k^\mu)^2]$ [3].

3. Numerical results and discussions

Shown in Fig. 1 are the energies of the ground state (a) and first excited state (b) obtained at $T = M = 0$ within several approximations as well as by exactly diagonalizing the pairing Hamiltonian for the schematic model, which consists of Ω doubly-folded equidistant levels with the single-particle energies chosen as $\epsilon_k = k - (\Omega + 1)/2$ MeV. The displayed results are for the half-filled case with $N = \Omega = 10$, and plotted as functions of the pairing interaction parameter G . It is seen that the LNSQRPA describes rather well the exact energies of both the ground and first excited states without any discontinuity in the region around G_c , where all other approaches such as the RPA, QRPA, and SCQRPA collapse.

The level-weighted gap, total energy, and heat capacity obtained for the systems with $N = \Omega = 10$ and 50 are shown as functions of temperature T in Fig. 2. Beside the predictions by the SCQRPA, LNSQRPA, as well as by their corresponding limits, FTBCS1 and FTLN1, where coupling to QRPA is omitted (i.e. n_k is described by the Fermi-Dirac distribution for free fermions), and the finite-temperature (FT) BCS results, the exact CE results are also shown. This figure clearly demonstrates how QNF smooth out the sharp SN phase transition in finite systems. The pairing gap never collapses, but decreases monotonously with increasing T , whereas the spike at T_c in the heat capacity, which serves as a signature of sharp SN phase transition within the FTBCS, becomes strongly depleted to a broad bump.

At finite angular momentum $M \neq 0$, the FTBCS theory predicts the Mottelson-Valatin effect, according to which, the zero-temperature pairing gap decreases with increasing M and collapses at $M = M_c$ because the angular momentum blocks the levels close to the Fermi surface [Fig. 3 (a) and 3 (c)]. Thermal effects relax the blocking, opening some levels around the Fermi surface for pairing. This leads to the thermally assisted pairing gap (or pairing reentrance), according to which at a certain $T = T_1$ the pairing gap becomes finite even at $M > M_c$ [7, 8]. With increasing

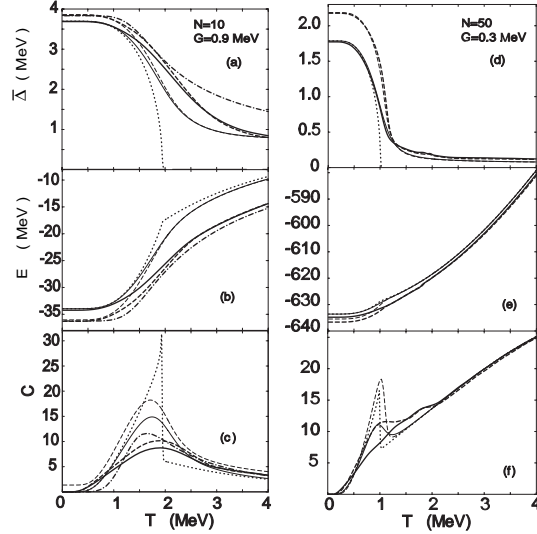


Figure 2. Level-weighted pairing gap $\bar{\Delta}$, total energy E , and heat capacity C , as functions of T for $N = \Omega = 10$ (a - c) and 50 (d - f) obtained within the FTBCS (dotted), FTBCS1 (thin solid), FTLN1 (thin dashed), SCQRPA (thick solid), LNSCQRPA (thick dashed). The dash-dotted lines for $N = 10$ are the exact CE results.

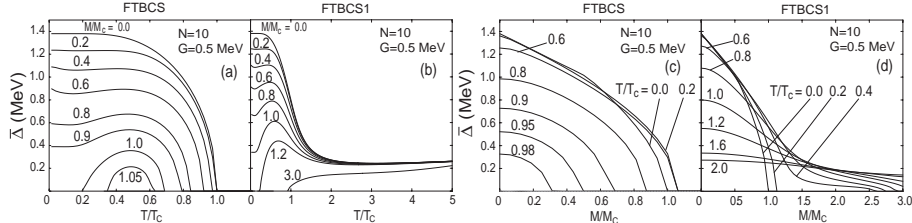


Figure 3. Level-weighted pairing gaps $\bar{\Delta}$ for $N = \Omega = 10$ as a functions of temperature T at various values of M/M_c and angular momentum M at various values of T/T_c within the FTBCS (a, c) and FTBCS1 (b, d) theories.

T thermal effects again break the pairs so that the gap disappears at $T = T_2 > T_1$ [See Fig. 3 (a) for $M/M_c \geq 1$]. In finite systems, the QNF smooth out both the Mottelson-Valatin transition and thermal assisted pairing, for instance, for $N = \Omega = 10$ with $G = 0.5$ MeV at $T/T_c \geq 1$, the gap only decreases monotonously with increasing M but never vanishes [See Fig. 3 (d) for $M/M_c \geq 1$], whereas at $M/M_c \geq 3$, the pairing gap reappears at $T > T_1$ but remains finite with further increasing T [See Fig. 3 (b) for $M/M_c \geq 3$].

The odd-even mass difference contains the admixture with the contribution from uncorrelated single-particle configurations, which increases with T . Therefore, the simple extensions of this formula to obtain the three-point and four-point gaps, in principle, do not hold at finite temperature. We propose an improved odd-even mass difference formula at $T \neq 0$, namely

$$\tilde{\Delta}^{(3)}(\beta, N) = \frac{G}{2} \left[(-1)^N + \sqrt{1 - 4 \frac{S'}{G}} \right], \quad S' = \frac{1}{2} [\langle \mathcal{E}(N+1) \rangle_\alpha + \langle \mathcal{E}(N-1) \rangle_\alpha] - \langle \mathcal{E}(N) \rangle_\alpha^{(0)}, \quad (6)$$

where $\langle \mathcal{E}(N) \rangle_\alpha$ is the total energy of the system with N particles within the grand canonical ensemble (GCE) ($\alpha = \text{GC}$) or CE ($\alpha = \text{C}$); $\langle \mathcal{E} \rangle_\alpha^{(0)} \equiv 2 \sum_k [\epsilon_k - G f_k^{(\alpha)} / 2] f_k^{(\alpha)}$ with $-G \sum_k [f_k^{(\alpha)}]^2$

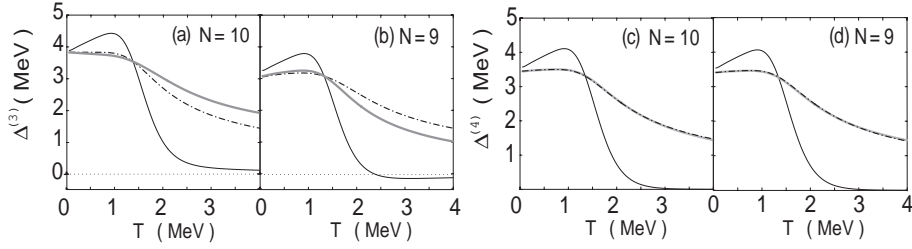


Figure 4. Pairing gaps extracted from the odd-even mass differences as functions of T for $N = 10$ (a,c) and $N = 9$ (b,d) ($\Omega = 10$, $G = 0.9$ MeV). The thin solid and thick solid lines denote the gap $\Delta^{(3)}(N)$ ($\Delta^{(4)}(N) = [\Delta^{(3)}(N) + \Delta^{(3)}(N-1)]/2$), and the improved gap $\tilde{\Delta}^{(i)}(\beta, N)$ ($i = 3, 4$) from Eq. (6), respectively. The dash-dotted lines are the canonical gaps $\Delta_C^{(i)}$.

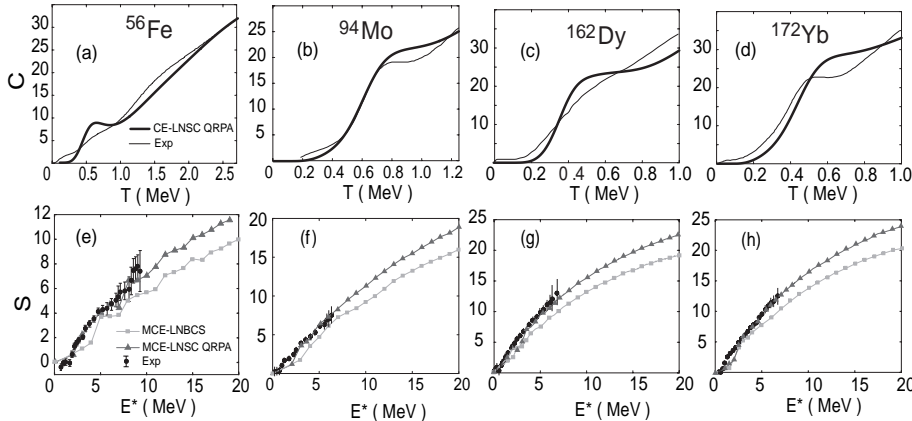


Figure 5. CE heat capacities C as functions of T and MCE entropies S as functions of excitation energy E^* for ^{56}Fe , ^{94}Mo , ^{162}Dy , and ^{172}Yb . Experimental data are taken from [11].

coming from uncorrelated single-particle configurations. Shown in Fig. 4 are the pairing gaps $\Delta^{(i)}(\beta, N)$ ($i = 3$ and 4), obtained for $N = 9$ and 10 ($\Omega = 10$) by using the simple extension of the odd-even mass formula to $T \neq 0$ as well as the modified gaps $\tilde{\Delta}^{(i)}(\beta, N)$ from Eq. (6), and the canonical gaps $\Delta_C^{(i)}$. It is seen in Fig. 4 that the naive extension of the odd-even mass formula to $T \neq 0$ fails to match the temperature-dependence of the canonical gap $\Delta_C^{(i)}$. The gap $\Delta^{(3)}(\beta, N = 9)$ even turns negative at $T > 2.4$ MeV, suggesting that such simple extension of the odd-even mass difference to finite T is invalid. The modified gap $\tilde{\Delta}^{(i)}(\beta)$ is found in much better agreement with the canonical one, whereas the modified four-point gaps $\tilde{\Delta}^{(4)}(\beta)$ practically coincide with the canonical gaps. The comparison in Fig. 4 suggests that formula (6) is a much better candidate for the experimental gap at $T \neq 0$, rather than the simple odd-even mass difference.

In order to construct a feasible description for pairing within the CE, the eigenvalues of the LNBCS and LNSCQRPA, obtained for each total seniority S at $T = 0$, are embedded into the CE by using the partition function $Z_\gamma(\beta) = \sum_S d_S e^{-\beta \varepsilon_S^\gamma}$ ($\gamma = \text{LNBCS, LNSCQRPA}$). The resulting approaches are called the CE-LNBCS and CE-LNSCQRPA, respectively [10]. These solutions are also embedded into the microcanonical ensemble (MCE) by using the Boltzmann's definition for entropy, $S(\mathcal{E}) = \ln W(\mathcal{E})$, where $W(\mathcal{E})$ is the number of accessible states within

the energy interval $(\mathcal{E}, \mathcal{E} + \delta\mathcal{E})$. The corresponding approaches are called the MCE-LNBCS and MCE-LNSCQRPA, respectively [10].

The CE heat capacities and MCE entropies for several nuclei are shown in Fig. 5 as functions of T and excitation energy E^* , respectively. The single-particle energies are calculated within the deformed Woods-Saxon potentials. In order to have a consistent comparison with the recent experimental data in [11], we carried out calculations by using the CE-LNBCS and CE-LNSCQRPA for ^{56}Fe , where pairing is included within the complete $pf + g_{9/2}$ shell above the ^{40}Ca core. For Mo isotopes, pairing is included in the 22 degenerated single-particle levels above the ^{48}Ca core. For Dy and Yb the same is done on top of the ^{132}Sn core. It is clear from this figure that the CE-LNSCQRPA results agree quite well with the experimental data [11], which are also deducted from the CE. The MCE entropies, obtained within the MCE-LNBCS and MCE-LNSCQRPA using $\delta\mathcal{E} = 1$ MeV, are plotted versus the experimental data. It is seen that the MCE-LNSCQRPA entropy not only offers the best fit to the experimental data but also predicts the results up to higher $E^* > 10$ MeV.

4. Conclusions

The proposed LNSCQRPA theory can describe without discontinuity the pairing properties of hot noncollectively rotating nuclei at any values of pairing interaction parameter G , temperature T , and angular momentum M . In the limit of zero temperature and zero angular momentum, it offers the best fits to the exact solutions in the weak coupling region with large particle numbers for the energy of the first excited state, whereas the SCQRPA reproduces well the exact one in the strong coupling region. In the limit of very large G all the approximations predict nearly the same value as that of the exact one. Under the effect of QNF, the paring gaps obtained at different values M of angular momentum decrease monotonously as T increases, and do not collapse even at hight T . The effect of thermally assisted pairing (pairing reentrance) shows up in such a way that the pairing gap reappears at a given $T_1 > 0$ and remains finite at $T > T_1$, in qualitative agreement with the results of Ref. [9]. We suggest a novel formula to extract the pairing gap at $T \neq 0$ from the difference of total energies of even and odd systems, where the contribution of uncorrelated single-particle motion is subtracted. Its prediction is found in much better agreement with the canonical gap than the simple extension of the odd-even mass formula to $T \neq 0$. Finally, we embedded the solutions of the LNBCS and LNSCQRPA into the CE and MCE, and found that the CE-LNSCQRPA predictions are in quite good agreements with the exact results as well as the recent experimental data. The present approach can also describe simultaneously and self-consistently the experimentally extracted total energy, heat capacity, and entropy within both CE and MCE treatments. It is simple and feasible for the application to larger finite systems, where the exact matrix diagonalization and/or solving the Richardson equation are impracticable to find all eigenvalues, whereas other methods, such as the quantum Monte-Carlo calculations, are time consuming.

References

- [1] Volya A, Brown B A and Zelevinsky V 2001 *Phys. Lett. B* **509** 37.
- [2] Hung N Q and Dang N D 2009 *Phys. Rev. C* **79** 054328.
- [3] Hung N Q and Dang N D 2007 *Phys. Rev. C* **76** 054302; 2008 *Ibid.* **77** 029905(E).
- [4] Dang N D and Hung N Q 2008 *Phys. Rev. C* **77** 064315.
- [5] Lipkin H J 1960 *Ann. Phys. (NY)* **9** 272; Nogami Y 1965 *Phys. Lett.* **15** 4.
- [6] Hung N Q and Dang N D 2008 *Phys. Rev. C* **78** 064315.
- [7] Moretto L G 1971 *Nucl. Phys. A* **185** 145.
- [8] Balian R, Flocard H and Vénéroni M 1999 *Phys. Rep.* **317** 251.
- [9] Frauendorf S, Kuzmenko N K, Mikhajlov V M and Sheikh J A 2003 *Phys. Rev. B* **68** 024518.
- [10] Hung N Q and Dang N D 2010 *Phys. Rev. C* **81** 057302.
- [11] Melby E *et al.* 1999 *Phys. Rev. Lett.* **83** 3150; Guttormsen M *et al.* 2000 *Phys. Rev. C* **62** 024306; Schiller A *et al.* 2001 *Phys. Rev. C* **63** 021306(R); Algin E *et al.* 2008 *Phys. Rev. C* **78** 054321.